# Mechanisms of Strength, Thermal Stability, and Doping Effects in Metal-Doped Bilayer Borophene for Energy Storage Applications Using a DFT-Trained Deep-Learning Potential

Shin-Pon Ju[1,2*], An-Zhi Lin[1], Shan-Han Lo [1], Hui-Lung Chen[3]*, Hsin-Tsung Chen[4*], and Hsing-Yin Chen[2]

[1]Department of Mechanical and Electro-Mechanical Engineering, National Sun Yat-sen University, Kaohsiung 804, Taiwan

[2]Department of Medicinal and Applied Chemistry, Kaohsiung Medical University, Kaohsiung 80708, Taiwan

[3]Department of Chemical and Materials Engineering, Chinese Culture University, Taipei, 111, Taiwan

[4]Department of Chemistry R&D Center for Membrane Technology and Research Center for Semiconductor Materials and Advanced Optics, Chung Yuan Christian University, Chungli District, Taoyuan City 320314, Taiwan

*Corresponding author: (Shin-Pon Ju: jushin-pon@mail.nsysu.edu.tw, Hui-Lung Chen (chl3@ulive.pccu.edu.tw), Hsin-Tsung Chen (htchen@cycu.edu.tw)

Table S1. DFT simulation parameters used in Quantum ESPRESSO for bilayer borophene.

| Parameter type | Setting or value |
|---|---|
| Calculation type | NPT or SCF |
| Pressure (Kbar) | 0 |
| Temperature (K) | 50~1000 K |
| Number of ionic steps | 200 |
| time step size (fs) | 1 |
| Kinetic energy cutoff (Ry) for wavefunctions | 40 |
| Kinetic energy cutoff (Ry) for charge density and potential | 320 |
| Convergence criterion of self-consistent calculation, (Ry) | $2 \times 10^{-5}$ |
| Pseudopotential (version) | SSSP efficiency (V1.30) |
| K-point setting level using Materials Cloud | Normal |

Table S2. Parameter settings for DeePMD DLP training

| Parameter | Value |
|---|---|
| model descriptor | se_a |
| rcut, Å | 6 |
| rsmth, Å | 5.8 |
| embedding neural network | {25, 50, 100} |
| fitting neural network | {240, 240, 240} |
| DPGEN models | 4 |
| training step for label process/final training | $1*10^6$/$2.5*10^6$ |
| $P_e^{start}$ (starting energy weight) | 1 |
| $P_e^{limit}$ (final energy weight) | 1 |
| $P_f^{start}$ (starting force weight) | 1000 |
| $P_f^{limit}$ (final force weight) | 1 |

Table S3. Atomic structures employed in the DFT calculations at 50 K and 300 K. Since reference b does not provide explicit structure names, the borophene configurations shown in the corresponding figure are adopted.

| Structure | Structural Type | Atoms |
|---|---|---|
| $\beta 12$ borophene[a] | Single-layer borophene | 15 |
| x3 bigophone | | 20 |
| striped borophene[a] | | 16 |
| Borophene(Fig.1a)[b] | Bilayer Borophene | 32 |
| Borophene(Fig.1c)[b] | | 16 |
| Borophene(Fig.1e)[b] | | 16 |
| Borophene(Fig.1f)[b] | | 8 |
| Borophene(Fig.5i)[b] | | 30 |
| Borophene(Fig.5j)[b] | | 60 |
| Borophene(Fig.5k)[b] | | 60 |
| Borophene(Fig.5m)[b] | | 62 |
| Borophene(Fig.5n)[b] | | 14 |
| Borophene(Fig.5o)[b] | | 28 |
| Borophene(Fig.5p)[b] | | 28 |
| Borophene(Fig.5s)[b] | | 56 |
| Borophene(Fig.5t)[b] | | 16 |

a: Peng, Bo, et al. Stability and strength of atomically thin borophene from first principles calculations. Materials Research Letters, 2017, 5.6: 399-407.

b: Gao, Nan, et al. Structure and stability of bilayer borophene: The roles of hexagonal holes and interlayer bonding. FlatChem, 2018, 7: 48-54.

Table S4. Structures used in the DFT calculations. The simulations were performed at 300 K.

| Structure | Structural Type | Atoms |
|---|---|---|
| p6m2 borophene[a] | | 64 |
| p6m2 borophene[a] | | 64 |
| p6m2 borophene[a] | | 16 |
| p6m2 borophene[a] | Bilayer Borophene | 16 |
| p6mmm borophene[a] | | 18 |
| p6m2 borophene[a] | | 16 |
| p6mmm borophene[a] | | 18 |

[a]Gao, Nan, et al. Density functional theory study of bilayer borophene-based anode material for rechargeable lithium ion batteries. Langmuir, 2023, 39.29: 10270-10279.

Table S5. Structures used in the DFT calculations. The simulations were performed at five different temperatures: 300 K, 400 K, 500 K, 600 K and 1000 K.

| Structure | Structural Type | Atoms |
|---|---|---|
| p6m2 borophene (Al doping) | Metal-doped bilayer | 64 |
| p6m2 borophene (Ru doping) | | 64 |
| p6mmm borophene (Al doping) | | 72 |
| p6mmm borophene (Ru doping) | | 72 |

Table S6. Structures used in the DFT calculations. The simulations were performed at six different temperatures: 50 K, 300 K, 400 K, 500 K, 600 K and 1000 K.

| Formula | Structure | Atoms |
|---|---|---|
| p6m2 borophene[c] | Bilayer Borophene | 16 |
| p6mmm borophene[c] | | 18 |

Table S7. Configuration-averaged nearest-neighbor bond lengths for B–B, B–Al, and B–Ru pairs in pristine and doped p6m2 and p6mmm bilayers. Values are obtained from relaxed structures by averaging over all first-neighbor pairs. ΔL(B–X) denotes the bond-length mismatch, defined as the difference between the dopant–boron bond length (B–Al or B–Ru) and the average B–B bond length in the same configuration.

| Configuration | Average bond length (Å) | | | ΔL(B-X)[a] (Å) |
|---|---|---|---|---|
| | B-B | B-Al | B-Ru | |
| **p6m2 (pristine)** | 1.7384 | — | — | — |
| p6m2-Al(0.8 at.%) | 1.7340 | 2.1566 | — | +0.4226 |
| p6m2-Al(1.6 at.%) | 1.7324 | 2.1560 | — | +0.4236 |
| p6m2-Ru(0.8 at.%) | 1.7333 | — | 2.1642 | +0.4309 |
| p6m2-Ru(1.6 at.%) | 1.7329 | — | 2.1622 | +0.4293 |
| **p6mmm (pristine)** | 1.8399 | — | — | — |
| p6mmm-Al(1.05 at.%) | 1.8002 | 2.1553 | — | +0.3551 |
| p6mmm-Al(2.1 at.%) | 1.7929 | 2.1562 | — | +0.3633 |
| p6mmm-Ru(1.05 at.%) | 1.8017 | — | 2.1649 | +0.3632 |
| p6mmm-Ru(2.1 at.%) | 1.7957 | — | 2.1629 | +0.3672 |

Table S8. Interlayer bond dissociation energies for pristine and doped p6m2 and p6mmm bilayers, evaluated from the energy difference between the intact bilayer and two isolated single layers separated by a distance much larger than the DLP cutoff. For each configuration, the total energy difference ΔE between the bound bilayer and the non-interacting monolayers is divided by the number of CN7-mediated interlayer bonds $N_{\mathrm{bond}}$to obtain the per-bond dissociation energy $E_{\mathrm{diss}}^{(\mathrm{per\ CN7})}$. The table lists the total number of interlayer bonds, the numbers of B–X and B–B interlayer bonds, and the corresponding $E_{\mathrm{diss}}^{(\mathrm{per\ CN7})}$ values.

| **Configuration** | **interlayer bonds** | **B-X(Al/Ru) bonds** | **B-B bonds** | $E_{\mathrm{diss}}^{(\mathrm{per\ CN7})}$ **(eV/bonds)** |
|---|---|---|---|---|
| pristine_p6m2 | 1260 | 0 | 1260 | 0.94 |
| p6m2-Al(0.8 at.%) | 1260 | 90 | 1170 | 0.89 |
| p6m2-Al(1.6 at.%) | 1260 | 180 | 1080 | 0.89 |
| p6m2-Ru(0.8 at.%) | 1260 | 90 | 1170 | 0.84 |
| p6m2-Ru(1.6 at.%) | 1260 | 180 | 1080 | 0.80 |
| pristine_p6mmm | 4322 | 0 | 4322 | 1.29 |
| p6mmm-Al(1.05 at.%) | 4322 | 144 | 4178 | 1.28 |
| p6mmm-Al(2.1 at.%) | 4322 | 288 | 4034 | 1.23 |

| | | | | |
|---|---|---|---|---|
| p6mmm-Ru(1.05 at.%) | 4322 | 144 | 4178 | 1.03 |
| p6mmm-Ru(2.1 at.%) | 4322 | 288 | 4034 | 0.73 |

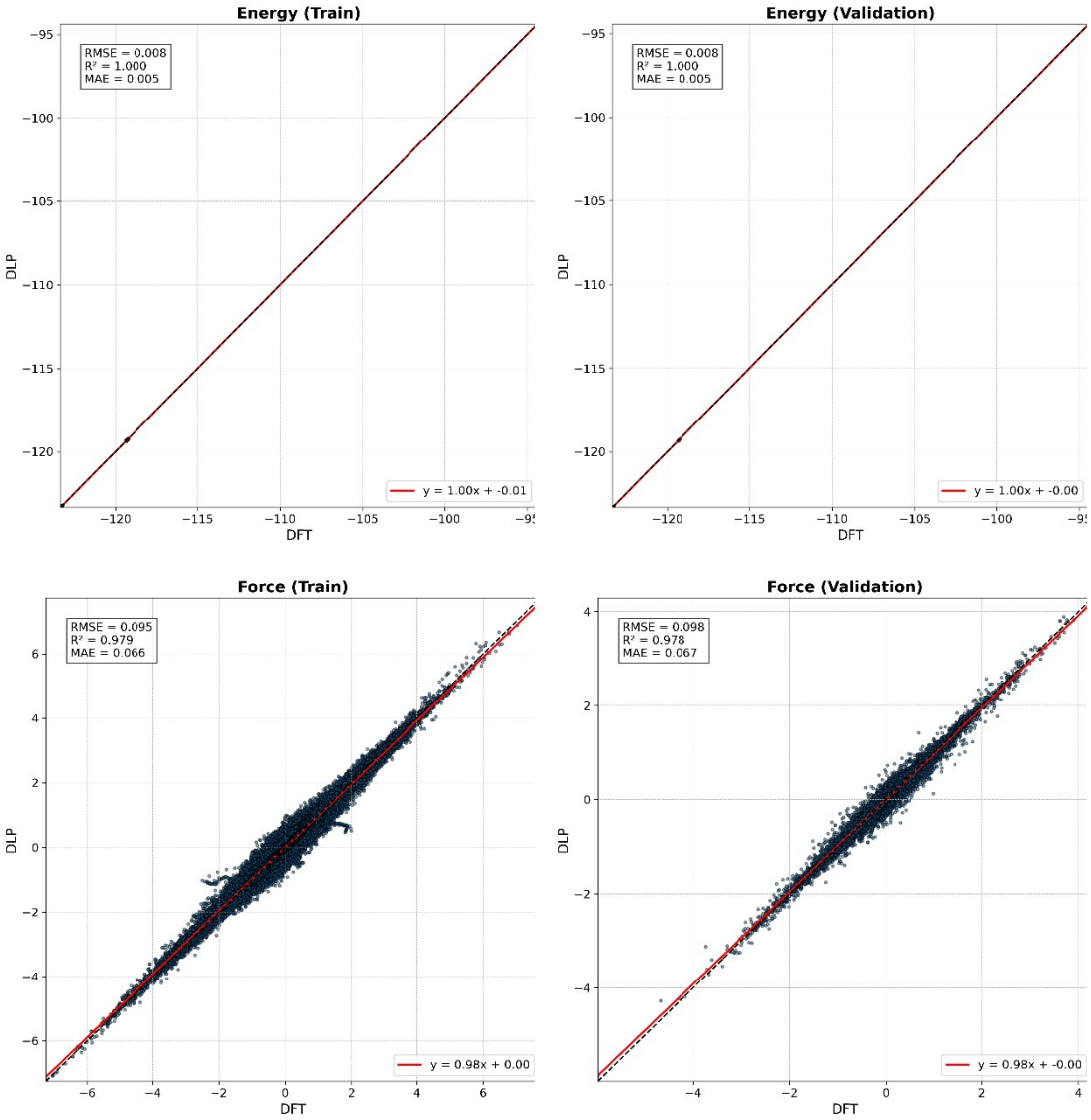


Figure S1. Correlation between DLP and DFT predictions for system energies and atomic forces. Results are shown for the training set (95%) and validation set (5%). Black lines represent the ideal y = x correlation, while red lines indicate linear regression fits. Energy is in eV/atom and force in eV/Å.

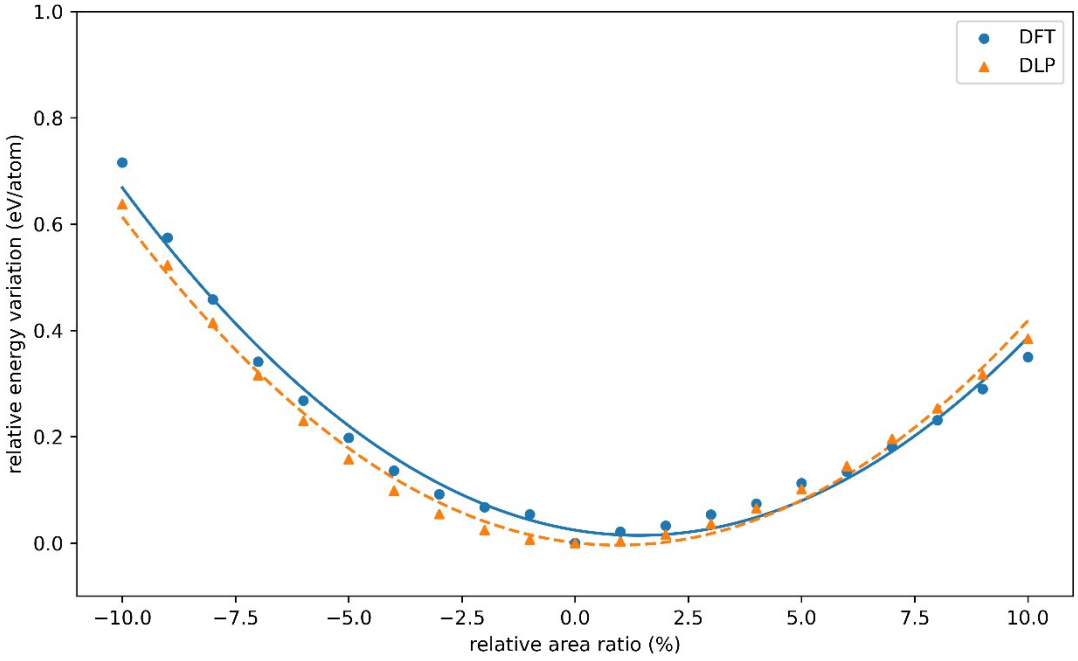


(a)

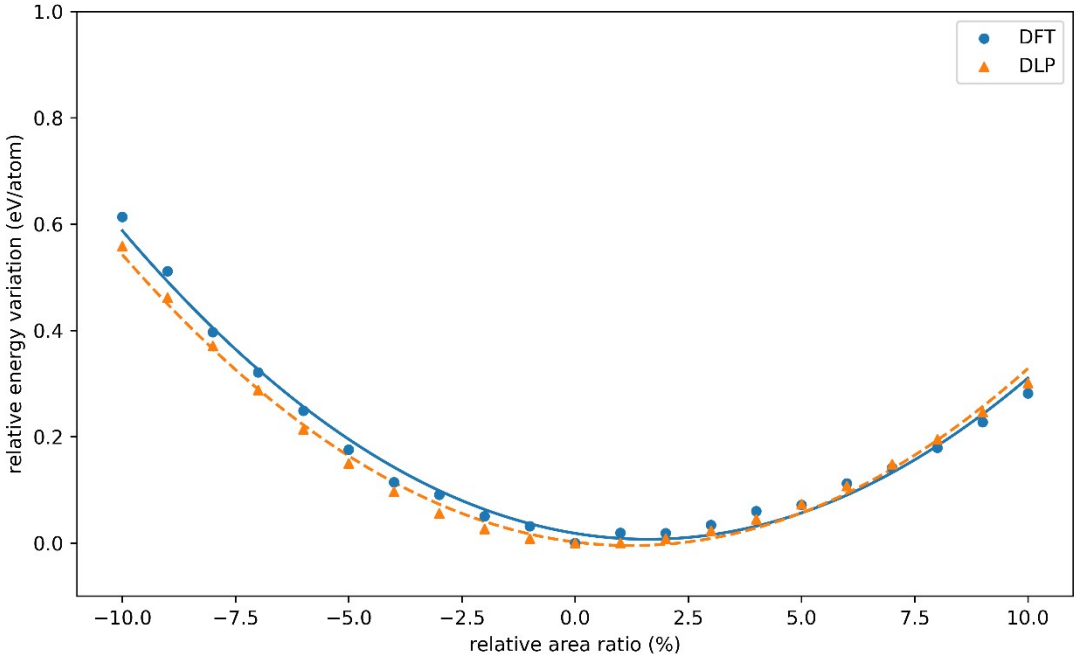


(b)

Figure S2. Energy-area curves for bilayer borophene structures calculated using DLP and DFT: (a)p6m2-Al(0.8 at.%) and (b)p6m2-Ru(0.8 at.%). The relaxed configurations at 0% strain serve as reference states. Structures were uniformly scaled in both x and y directions.